Results in Physics 10 (2018) 118–125

Contents lists available at ScienceDirect

Results in Physics

journal homepage: www.elsevier.com/locate/rinp

Analysis of Carreau fluid in the presence of thermal stratification and magnetic field effect

S. Bilal[b,c,*], Shafqatullah[b], Ali Saleh Alshomrani[a], M.Y. Malik[a], Nabeela Kausar[c], Farzana Khan[b], Khalil-ur-Rehman[b]

[a] Department of Mathematics, King Abdulaziz University, Jeddah 21589, Saudi Arabia
[b] Department of Mathematics, Quaid-i-Azam University, Islamabad 44000, Pakistan
[c] Department of Mathematics, AIR University, E9 Islamabad 44000, Pakistan

ARTICLE INFO

Keywords:
Carreau fluid
Magnetic field
Thermal stratification
Shooting algorithm
Stretching cylinder

ABSTRACT

In current article theoretical analysis is executed to examine flow features of Carreau fluid by conferring scintillating aspects of thermal stratification. Flow field equations are attained by incorporating infinite shear rate viscosity and magnetic field effects. Afterwards, the partial differential obtained from the fundamental laws of continuity, momentum and energy containing stratification aspects are attained. These consequent partial differential expressions are so intricate that it seems difficult to solve analytically. Therefore Prandtl layer approximation is capitalized to retain efficient parts of flow narrating differential equations. Then next step is to eradicate the in active parts of partial equations by implementing transformations. The solution structured of reduced system is acquired by self-coded shooting algorithm. The variation in physical profiles with respect to involved parameters is exhibited with the aid of graphs and tables. It is inferred that Carreau fluid behaves in opposite pattern for $n > 1$ (shear thickening) and $n < 1$ (shear thinning) liquid. It is also depicted that thermal stratification delineates the thermal distribution of fluid flow.

Introduction

Technology driven world compels the researchers to work out in the investigation of non-Newtonian liquids. Thus the highly motivated researchers are taking keen interest in the study of non-Newtonian fluid rheology due to practical applicability in various industrial procedures and daily routine processes. As the non-Newtonian fluid material expresses the complex mathematical and physical relation between shear stress and shear rate so they are categorized into shear thinning, shear thickening and dilatant materials. Although various fluid models are introduced in this regards to scrutinize the intrinsic features of above materials but no single model is found in this regard. At last the endeavor made by P.J. Carreau (1972) [1] came into action and proposed the model of Carreau fluid. He described that Carreau fluid model or generalized Newtonian fluid is the combination of power law model and Newtonian fluid model which is capable of expressing shear thinning features at low shear rate and shear thickening properties at higher shear rate. Various notable investigation of Carreau fluid model in different physical frameworks and associated flow restrictions are conducted by following recommendable researcher. Few of them are as follows. Olajuwan [2] remarked that constitutive expression of Carreau fluid reduced to Newtonian fluid by increasing deformation rate. Pantokratoras [3] explained Carreau model by using controlling parameter n. He described that Carreau fluid depicts the properties of shear thinning material for $0 < n < 1$ and as shear thickening for $n > 1$. Shadid and Eckert [4] examined dissipative effect on Carreau fluid caused by a stretched cylinder. Thermophysical features of Carreau fluid in an annular space between two concentric cylinders were presented by Khellaf and Lauriat [5]. The interrogation on the impact of non-linear radiation in the flow of Carreau fluid was conducted by Raju and Sandeep [6]. Magnetohydrodynamic boundary layer flow of Carreau fluid due to a stretchable surface was depicted by Khan and Hashim [7]. Akbar et al. [8] computed dual solution of MHD stagnant flow of Carreau fluid due to a stretching sheet. The past and future developments in this direction is accessed through [9–12].

Stratification is a convective thermal transport phenomenon arises due to deposition of particles having variant densities and temperature among the layers. In recent fast technologically growing years the examination of stratified flow with various field conditions has received overwhelming attention in research community. These applications involve thermal stratification of hydral reservoirs and oceans, heterogeneous mixtures in atmosphere, industrial food and manufacturing

* Corresponding author at: Department of Mathematics, AIR University, E9 Islamabad 44000, Pakistan.
E-mail address: smbilal@math.qau.edu.pk (S. Bilal).

https://doi.org/10.1016/j.rinp.2018.05.005
Received 28 January 2018; Received in revised form 15 April 2018; Accepted 2 May 2018
Available online 29 May 2018

Nomenclature

u, v	Velocity components	k	Thermal conductivity
ρ	Fluid density	ν^*	Kinematic viscosity
μ	Dynamic viscosity	c_p	Specific heat at constant pressure
K	Curvature parameter	A_1	First Rivlin-Erickson tensor.
$T_w(x)$	Prescribed surface temperature		Cauchy stress tensor
T_0	Reference temperature	$T_\infty(x)$	Variable ambient temperature
L^*	Reference length	U_0	Free stream velocity
$f'(\eta)$	Velocity of fluid	$f(\eta)$	Dimensionless variable
α	Thermal diffusivity	S	Thermal stratification parameter
τ	Extra stress tensor	Pr	Prandtl number
$\frac{d}{dt}$	material time derivative	$\Gamma > 0$	time constant
a, b	Positive constants	R	Radius of cylinder
		We	Weissenberg number
		Re_x	Reynolds number

processes and salinity stratification phenomenon in estuaries, rivers, and ground water reservoirs. Aspects of stratification in various non-Newtonian fluids were investigated in recent years by a lot of researchers. For sake of conciseness few of them are mentioned as follows. Srinivasacharya and Surender [13] interpreted the aspects of thermal and solutal stratification in boundary layer mixed convection flow towards a stretching sheet saturated with porous medium. Mishra et al. [14] reported the features of heat generation/absorption in double stratified flow of micropolar fluid in the attendance of Lorentz field. Reddy et al. [15] studied thermally stratified nanofluid flow over a stretching sheet saturated with non-Darcy porous medium. Variation in properties of nanomaterial liquid with the inclusion of stratification phenomenon was disclosed by Ibrahim and Makinde [16]. Abbasi et al. [17] executed the nature of doubly stratified Maxwell nanoliquid flow through series solutions. Hayat et al. [18] examined the nature of stratification effects for Maxwell liquid flow. Influences of double stratification and melting heat in stretched flow of Carreau and viscous nanoliquid are addressed by Farooq et al. [19,20].

The analysis of fluid flows with the interaction of magnetic field has engrossed substantive focus of investigators. Such considerations is due to its utilization in various mechanical, industrial and technological processes i.e. enhanced oil recovery, magnetohydrodynamic generators, electronic packages, pumps, thermal insulators, flow meters, power generation, etc. Furthermore, the appliance of magnetic field molds the orientation of interacting fluid molecules and also controls the intensity of flow phenomenon. Due to above mentioned importance researchers are considering fluid flows in various orientations under the effect of applied magnetic field. Few recent works in this direction is described as follows. Vajravelu et. al. [21] constituted a systematic study on axisymmetric flow of MHD viscous fluid through non isothermal stretching cylinder. They inspected that magnetic field parameter declines velocity and boundary layer thickness. Mukhopadhyay et al. [22] deliberated slip flow of MHD viscous fluid flow over a stretching cylinder. They predicted that magnetic field parameter and slip parameter decelerates velocity. Ibrahim [23] studied the magnetohydrodynamic flow through stretching sheet with convective boundary conditions.

The main objective of present investigation is twofold. First, is to construct mathematical modelling of Carreau fluid by considering infinite shear rate viscosity. Because Carreau fluid behave as shear thinning material for low shear rate viscosity and as shear thickening fluid for infinite shear rate viscosity. On the other hand second purpose is to evaluate the thermal features of Carreau fluid in the presence of stratification. From the accessed literature it is found that no such concept is available. So our purpose is to fill the gap.

Mathematical formulation

Two dimensional, steady, incompressible flow of Carreau fluid yield by stretching cylinder is considered. Fluid flow is along axial direction which is perpendicular to radial axis of cylinder as given in Fig. 1. Classical energy equation is incorporated which admits the role of thermal stratification. The Carreau fluid flow regime has interaction with perpendicularly applied magnetic field.

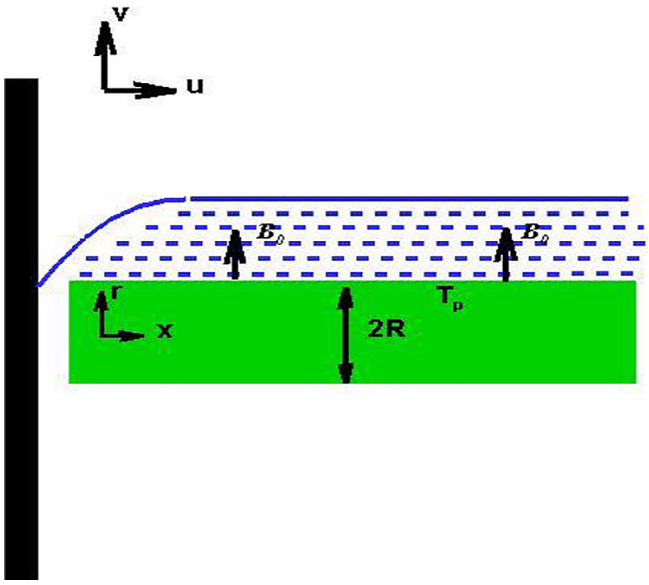

Fig. 1. Physical Configuration of Problem.

The flow model is controlled through trust worthy differential equations with the source of boundary layer approximation. The resultant boundary layer equations are:

$$\frac{\partial}{\partial x}(ru) + \frac{\partial}{\partial r}(rv) = 0, \tag{1}$$

$$u\frac{\partial u}{\partial x} + v\frac{\partial u}{\partial r} = \nu*\left(\frac{\partial^2 u}{\partial r^2} + \frac{1}{r}\frac{\partial u}{\partial r} + \frac{3\Gamma^2(n-1)}{2}\left(\frac{\partial u}{\partial r}\right)^2\frac{\partial^2 u}{\partial r^2} + \frac{\Gamma^2(n-1)}{2r}\left(\frac{\partial u}{\partial r}\right)^3\right) - \frac{\sigma B_0^2 u}{\rho}, \tag{2}$$

$$u\frac{\partial T}{\partial x} + v\frac{\partial T}{\partial y} = \frac{k}{\rho c_p}\left(\frac{1}{r}\frac{\partial T}{\partial r} + \frac{\partial^2 T}{\partial r^2}\right), \tag{3}$$

the associated boundary conditions are

$$u = u(x) = ax, v = 0, T_w(x) = T_0 + b\left(\frac{x}{l}\right) \text{ at } r = R, u \to 0, T \to T_\infty = T_0 + c\left(\frac{x}{l}\right) \text{ as } r \to \infty. \tag{4}$$

To report numerical solution first we have to step down the partial

differential equations given in Eqs. (2) and (3) into ordinary differential equations by using the set of transformation [22,24,25].

$$u = \frac{1}{r}\frac{\partial \psi}{\partial r}, \quad v = -\frac{1}{r}\frac{\partial \psi}{\partial x}, \quad \psi = \sqrt{u\nu^* x}Rf(\eta), \quad \eta = \frac{r^2-R^2}{2R}\sqrt{\frac{u}{\nu^* x}}, \quad \theta(\eta) = \frac{T-T_\infty}{T_w-T_\infty}, \tag{5}$$

By utilizing Eq. (5) into Eqs. (2) and (3), one can obtain the reduced form

$$(1+2K\eta)\frac{d^3f(\eta)}{d\eta^3} + f(\eta)\frac{d^2f(\eta)}{d\eta^2} - \left(\frac{df(\eta)}{d\eta}\right)^2 + 2K\frac{df(\eta)}{d\eta} + (We)^2K(1+2K\eta)\left(\frac{d^2f(\eta)}{d\eta^2}\right)^2 + \frac{3}{2}(n-1)(We)^2(1+2K\eta)\left(\frac{d^2f(\eta)}{d\eta^2}\right)^2\left(K\frac{d^2f(\eta)}{d\eta^2} + (1+2K\eta)\frac{d^3f(\eta)}{d\eta^3}\right) - M^2f'(\eta) = 0, \tag{6}$$

$$(1+2K\eta)\frac{d^2\theta(\eta)}{d\eta^2} + 2K\frac{d\theta(\eta)}{d\eta} + Pr\left(f(\eta)\frac{d\theta(\eta)}{d\eta} - \frac{df(\eta)}{d\eta}\theta(\eta) - S\frac{df(\eta)}{d\eta}\right) = 0, \tag{7}$$

while the reduced boundary conditions are

$$f(0) = 0, \quad \theta(0) = 1-S, \quad f'(0) = 1, \quad f'(\infty) = 0, \quad \theta(\infty) = 0, \tag{8}$$

here, the involved parameters are defined by

$$K = \frac{1}{R}\sqrt{\frac{L*\nu*}{U_0}}, \quad M = \sqrt{\frac{\sigma B_0^2 L*}{\rho U_0}}, \quad We = \Gamma\sqrt{\frac{U_0^3}{(L*)^3\nu*}}x, \quad \Pr = \frac{\mu c_p}{k} \quad \text{and} \quad S = \frac{c}{b}. \tag{9}$$

Here, K,M,We,Pr and S denotes curvature parameter, magnetic field parameter, Weissenberg number, Prandtl number and thermal stratification parameter. The detail of rest of involved quantities can be assessed in nomenclature.

The skin friction coefficient can be achieved by simple practice

$$C_f = \frac{\tau_w}{\rho\frac{U^2}{2}}, \text{with } \tau_w = \mu\left[\frac{\partial u}{\partial r} + \frac{\Gamma^2(n-1)}{\sqrt{2}}\left(\frac{\partial u}{\partial r}\right)^3\right]_{r=R}, \tag{10}$$

the relevant dimensionless form is

$$\sqrt{\mathrm{Re}_x}\,C_f = f''(0) + \frac{(We)^2(n-1)}{2}(f''(0))^3, \tag{11}$$

where, $Re_x = \frac{U_0x^2}{L\nu*}$ denotes local Reynolds number.

The local Nusselt number is defined as:

$$Nu_x = \frac{-xq_w}{k(T_w-T_0)}, q_w = -k\left(\frac{\partial T}{\partial r}\right)_{r=R}, \tag{12}$$

in dimensionless form it can be written as:

$$\frac{Nu_x}{\sqrt{Re_x}} = -\theta'(0). \tag{13}$$

Numerical procedure

The mathematical formulation of two dimensional Carreau fluid flows over a stretching cylinder comprises of intricate ordinary differential equations expressed in Eqs. (6) and (7) with end point condition given in Eq. (8). As the constructed system of equation is boundary value problem so for better depiction of solution we approach towards numerical simulation by implementing shooting technique chartered with Rk-Fehlberg (5th order) method. To accomplish this method we have to reduce the order of differential equation into initial value problem (IVP) by applying dummy substation.

$$f = \xi_1, f' = \xi_2, f'' = \xi_3, f''' = \xi_3', \theta = \xi_4, \theta' = \xi_5, \theta'' = \xi_5', \phi = \xi_6, \phi' = \xi_7, \phi'' = \xi_7', \tag{14}$$

By using Eq. (14), Eqs. (8) and (9) yield the following form

$$\xi_1' = \frac{df}{d\eta} = \xi_2, \tag{15}$$

$$\xi_2' = \frac{d^2f}{d\eta^2} = \xi_3, \tag{16}$$

$$\frac{d^3f}{d\eta^3} = X_3' = \frac{\xi_2^2 - \xi_1\xi_3 - 2K\xi_3(1+We^2\xi_3^2)^{\frac{n-1}{2}} - K(n-1)We^2\xi_3^3(1+We^2\xi_3^2)^{\frac{n-3}{2}} + M\xi_2}{(1+2K\eta)(1+We^2\xi_3^2)^{\frac{n-1}{2}} + (n-1)We^2\xi_3^2(1+2k\eta)(1+We^2\xi_3^2)^{\frac{n-3}{2}}}, \tag{17}$$

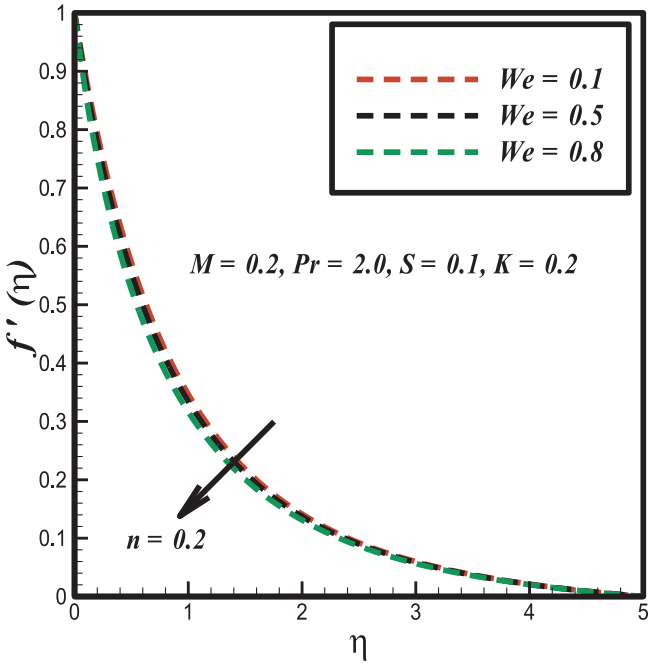

Fig. 2a. Effect of We on velocity profile for $n = 0.2$.

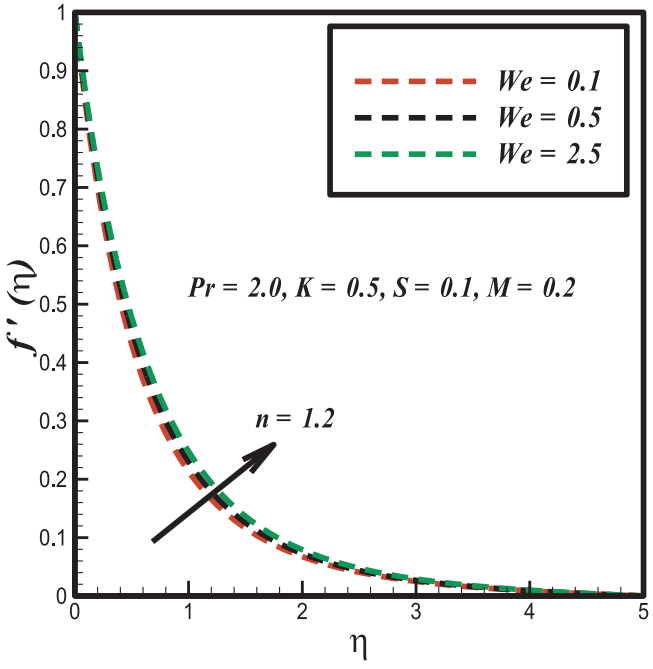

Fig. 2b. Effect of We on velocity profile for $n = 1.2$.

$$\xi_4' = \frac{d\theta}{d\eta} = \xi_5, \tag{18}$$

$$\xi_5' = \frac{d^2\theta}{d\eta^2} = \frac{-2K\xi_5 - \Pr(\xi_5\xi_1 - \xi_2\xi_4 - S\xi_1)}{(1 + 2K\eta)}, \tag{19}$$

the associated boundary conditions becomes

$$\xi_1(0) = 0, \xi_2(0) = 1, \xi_3(0) = \psi_1, \xi_4(0) = 1 - S, \xi_5(0) = 0. \tag{20}$$

Whereas, the far field conditions are transformed as

$$\xi_2(\infty) = 0, \quad \xi_4(\infty) = 0. \tag{21}$$

Now to solve Eqs. (15)–(19) along with boundary conditions Eq. (20) by shooting method we need the values of $\xi_3(0) = 1, \xi_5(0) = 1$ (i.e. initial approximation). Then the system of first order ODE's are solved with the help of Runge Kutta fifth order integration scheme.

Results and discussion

The purpose of this subsection is to interpret the influences of involved parameters on velocity field, temperature field, skin friction coefficient ($C_f \mathrm{Re}_x^{1/2}$) and Nusselt number ($N_u \mathrm{Re}_x^{-1/2}$). To achieve the desired output computational analysis is performed by implementing Matlab programmed Rk-Fehlberg code in combination with shooting scheme. It is worth mentioning to express that velocity profiles are elucidated for power law index i.e. $n < 1$ (Shear thinning fluid) and

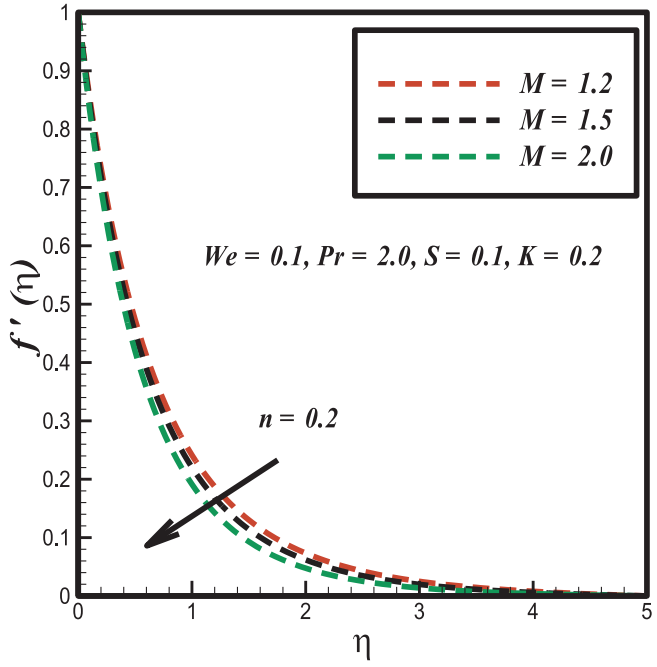

Fig. 3a. Effect of M on Velocity profile for $n = 0.2$.

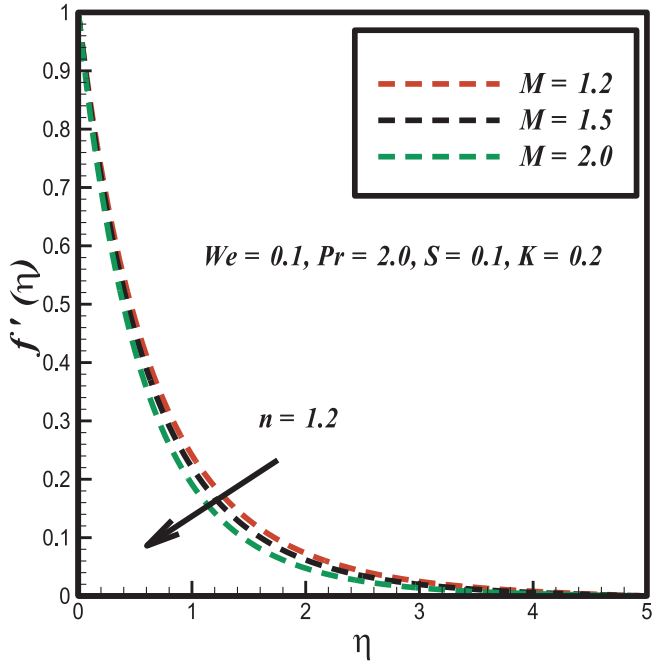

Fig. 3b. Effect of M on Velocity profile for $n = 1.2$.

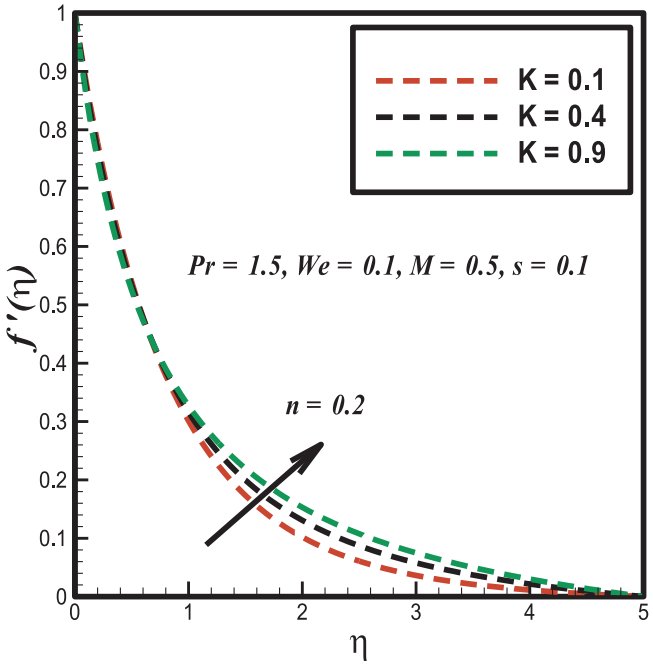

Fig. 4a. Effect of K on Velocity profile for $n = 0.2$.

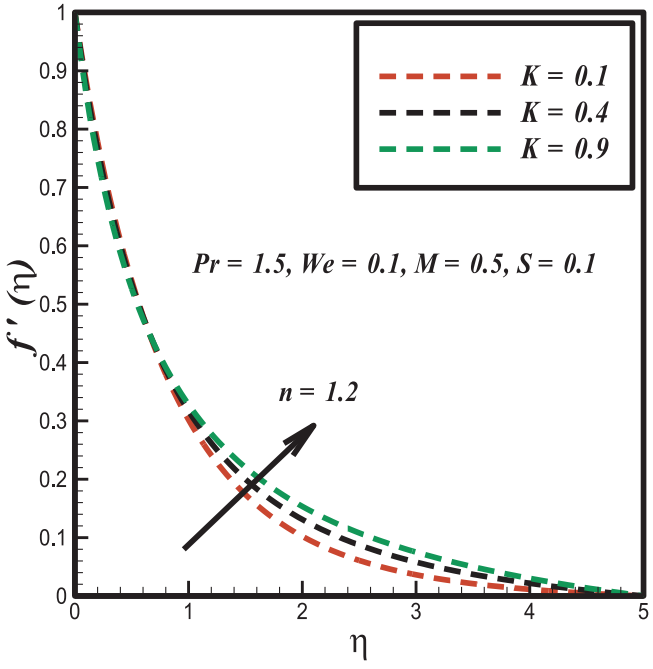

Fig. 4b. Effect of K on Velocity profile for $n = 1.2$.

$n > 1$ (Shear thickening fluid). Whereas, thermal profile is displayed for $S = 0$ (non-stratified medium) and (stratified medium). Here, we assigned realistic numerical values to other controlling parameters with a particular true objective to get knowledge about momentum and thermal fields.

This section is dedicated to describe the fluctuations in velocity, temperature, local skin friction coefficient, local Nusselt number through graphs and tables under different parametric conditions. Variation in velocity field with respect to inciting values of controlling parameters is revealed in Figs. 2–4.

Figs. 2a-b are elucidated to interpret the response of Weissenberg number (We) on fluid velocity for shear thinning ($n < 1$) and shear thickening ($n > 1$) cases. It is observed form the graphical sketch that intensifying values of Weissenberg number (We) bring accelerating attribute in velocity profile for shear thinning fluid ($n < 1$) whereas opposite pattern is depicted in case of shear thickening fluid ($n > 1$). The down surging behavior in Carreau fluid velocity for incrementing values of (We) is justified by the fact that by increasing (We) it yields enhancement in relaxation time of stressed fluid particles and hence more resistance is faced by these molecules which as an outcome disseizes the velocity. The impact of magnetic field parameter (M) on velocity profile for shear thickening and shear thinning cases is deliberated by way of Figs. 3a-b. From both frame works it is concluded that in both cases fluid velocity is decrementing function of magnetic field parameter (M). This pattern is due to higher magnitude of Lorentz

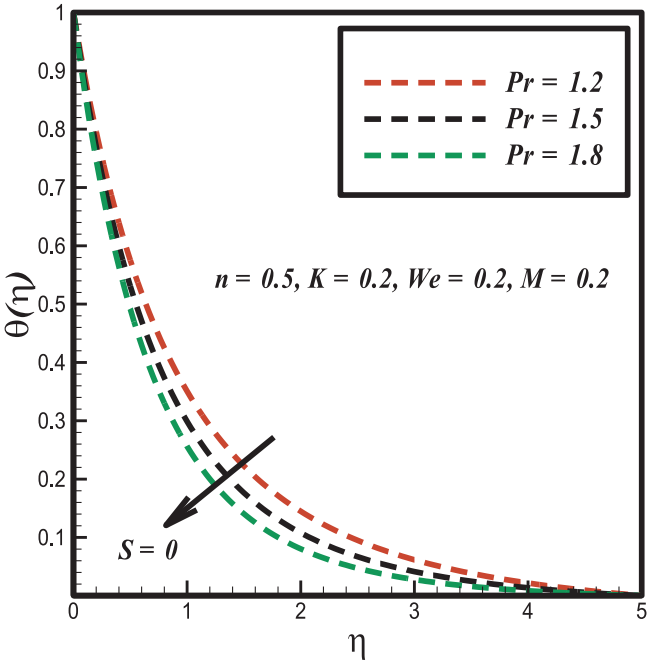

Fig. 5a. Effect of Pr on temperature profile for $S = 0.0$.

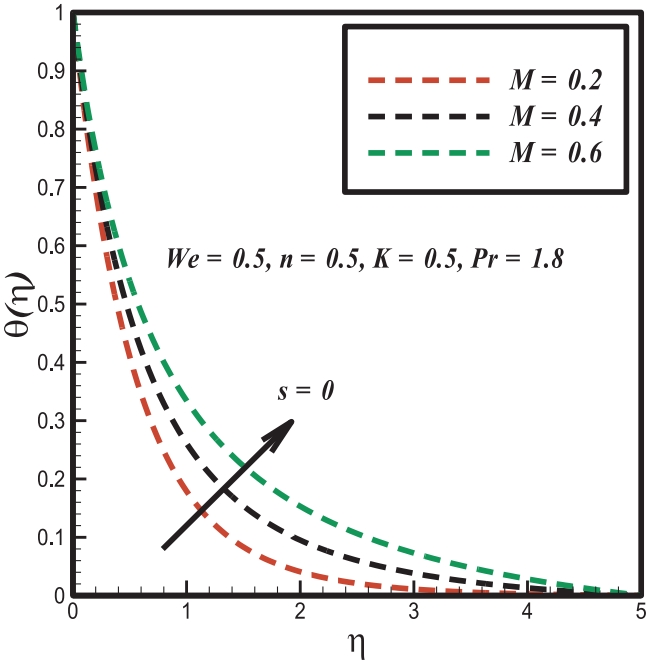

Fig. 6a. Effect of M on temperature profile for $S = 0.0$.

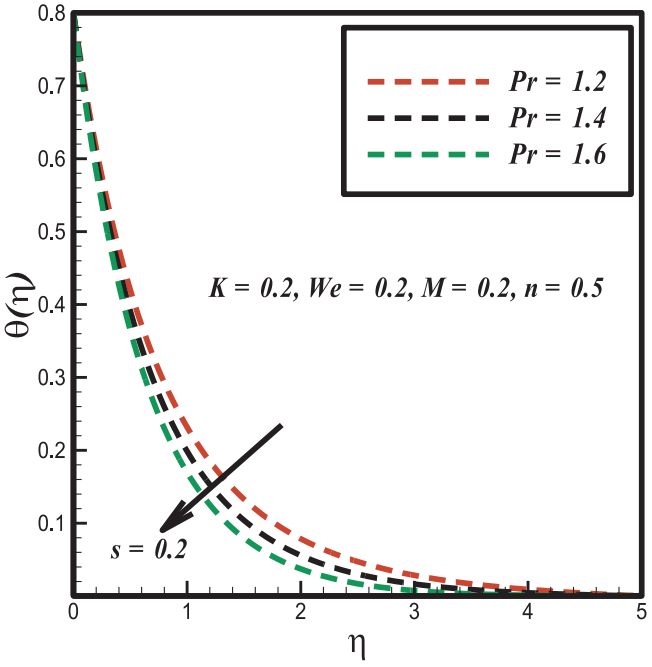

Fig. 5b. Effect of Pr on temperature profile for $S = 0.2$.

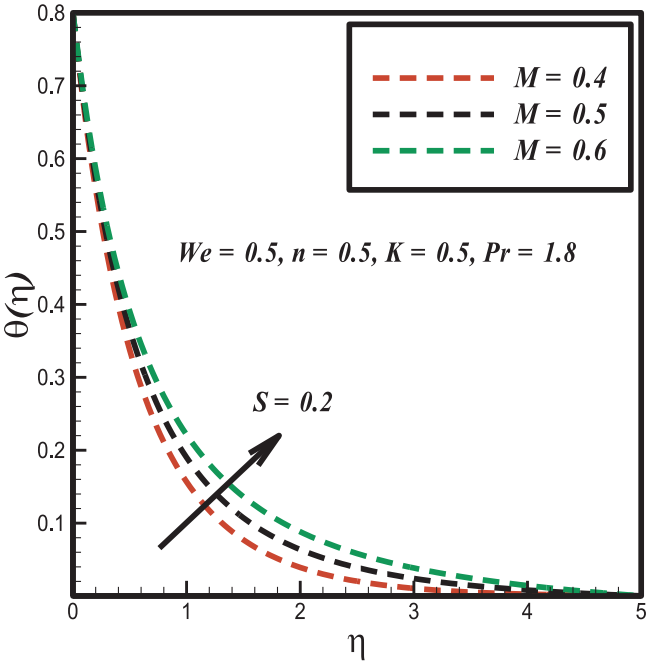

Fig. 6b. Effect of M on temperature profile for $S = 0.2$.

force resistive force come into action which causes fluid particle to flow in negative aptitude and as a consequence Carreau fluid particle diminishes. The attitude of velocity of Carreau fluid molecules for shear thinning and shearing thickening cases against increasing values of Curvature parameter (K) is disclosed in Figs. 4a-b. We choose $K = 0.1,0.2,0.3$ for better understanding and description of velocity pattern. In both sketches it is originated that velocity curves show positive pattern for inciting values of (K). As $K\ \alpha\frac{1}{R}$, so by increasing curvature parameter radius of cylindrical surface reduces as a result fluid contact with surface reduces and less resistance is encountered thus fluid particles accelerates in boundary layer. The variation in Carreau fluid molecules temperature with respect to involved parameter in the presence of stratification ($S = 0.2$) and in the absence of ($S = 0.0$) are elucidated with the help of Figs. 5–7. Figs. 5a-b. witnesses the reducing behavior of thermal distribution in response to progressive magnitude of Prandtl number (Pr) for stratification and non-stratification cases. This behavior is justified by the existence of inverse relation between the Prandtl number and Diffusion of thermal energy (i.e. transport of molecules in flow field due to temperature). Therefore rise in the magnitude of Prandtl number results signification declination in thermal field of Carreau fluid. Importance of magnetic field parameter on temperature profile for stratification and non-stratification cases is presented in Figs. 6a-b. Significantly improvement in $\theta(\eta)$ is observed for (M). As the magnetic field force contains resistive nature so it to decline the velocity of fluid particles. This decrease in velocity of fluid molecules enhances the resistive force among them and

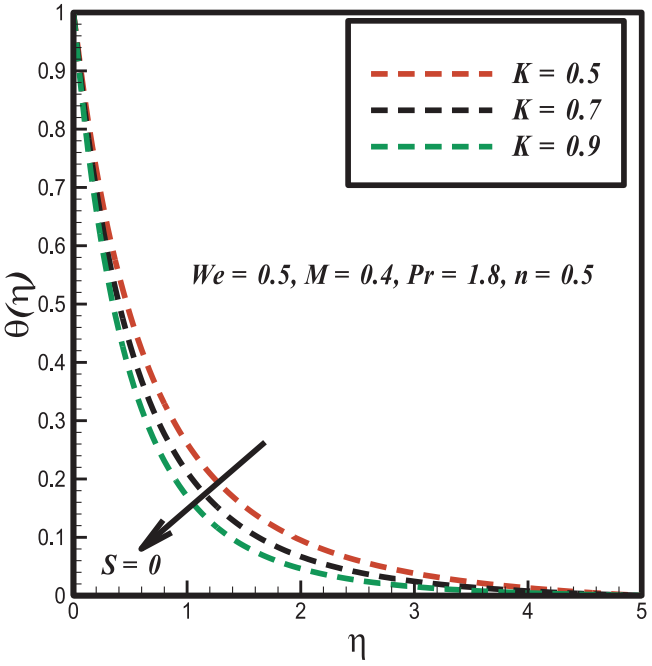

Fig. 7a. Effect of K on temperature profile for $S = 0.0$.

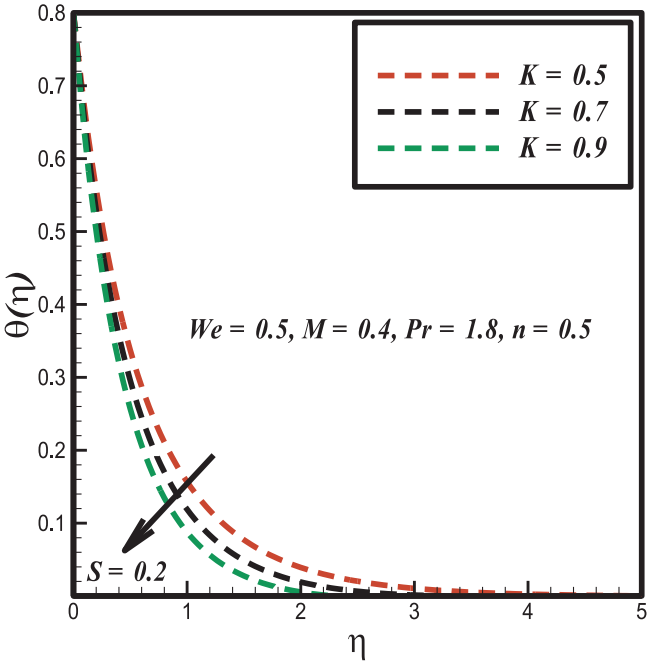

Fig. 7b. Effect of K on temperature profile for $S = 0.2$.

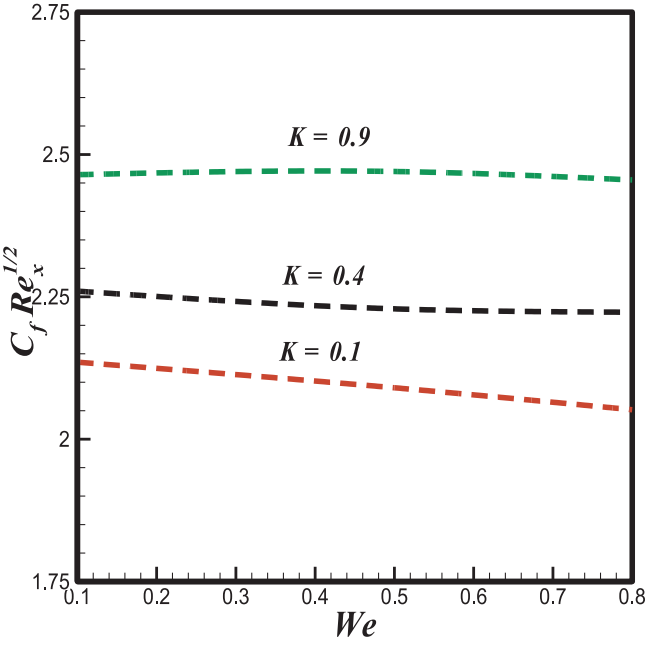

Fig. 8a. Fluctuation in Skin friction due to *We and K*.

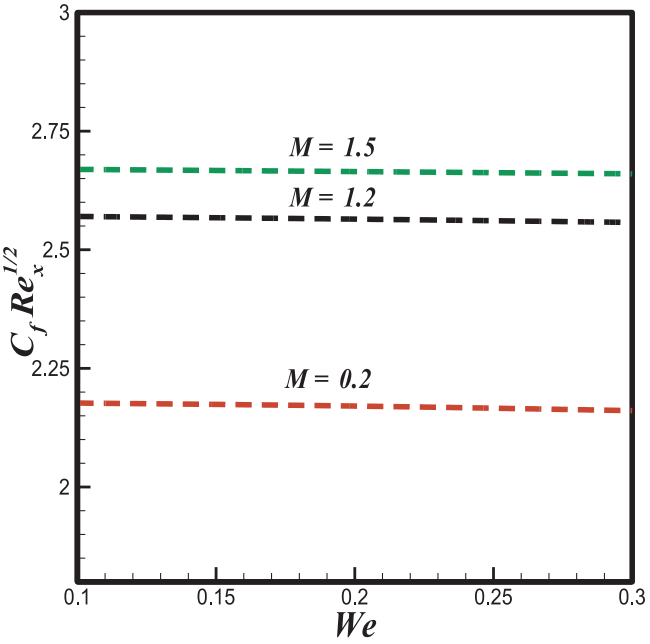

Fig. 8b. Fluctuation in Skin friction due to *M and We*.

as an outcome temperature of Carreau fluid molecules inclines. Figs. 7a-b illustrate the characteristics of curvature parameter (K) on thermal field. Here $\theta(\eta)$ shows positive response for (K). As the curvature parameter induces positive pattern in velocity of fluid molecules so this behavior yields the increment in average kinetic energy of molecules which is the measure of temperature. Thus fluid temperature increases for curvature parameter (K). The fluctuation in skin friction coefficient ($C_f Re_x^{1/2}$) is for inciting values of magnetic field parameter (M), Weissenberg number (We) and curvature parameter (K) is depicted in Figs. 8a-b. It can be explicitly observed from the portray that curvature parameter (K) and magnetic field (M) parameter enhances the amount of drag force whereas reverse pattern in found in case of variation in Weissenberg number (We). From the vertical axis of both sketches it is seen that we are describing the progressive attitude of skin friction coefficient in absolute sense. As the measure of Nusselt number is measure of heat transfer so the role of Nusselt in the characterization of problem is compulsory. Figs. 9a-b are sketched to study the influences of effecting parameter on convective heat transfer coefficient. From the graphical display it can be seen that (Pr) and (K) causes enhancement in Nusselt number whereas declined attitude is observed for magnetic field parameter (M). The reason for enhancement in magnitude of heat transfer rate for mounting values of (Pr) is justified by the ratio between momentum to thermal diffusivity express by Prandtl number (Pr). So by increasing (Pr) momentum diffusivity enriches and average kinetic motion of fluid particles fastens which as an outcome increases the heat transfer rate. More over the variation exhibited by various parameters on skin friction coefficient and Nusselt number are also justified by tabular data which is expressed in Tables 1–2. Table 1 describes numerical variation in drag force coefficient with respect to Weissenberg number (We) and magnetic field parameter (M) for cylindrical surface ($K = 0.5$) and Flat surface ($K = 0.0$). From the numerical data it can be analyzed that wall shear stress in case of flat surface is more apparent than cylinder. Table 3 shows the trifling change in Nusselt number $\left(\frac{Nu}{Re_x^{\frac{1}{2}}}\right)$ for sheet and cylinder. It can be explicitly observed that coefficient of convective heat transfer is more in case of cylinder than sheet.

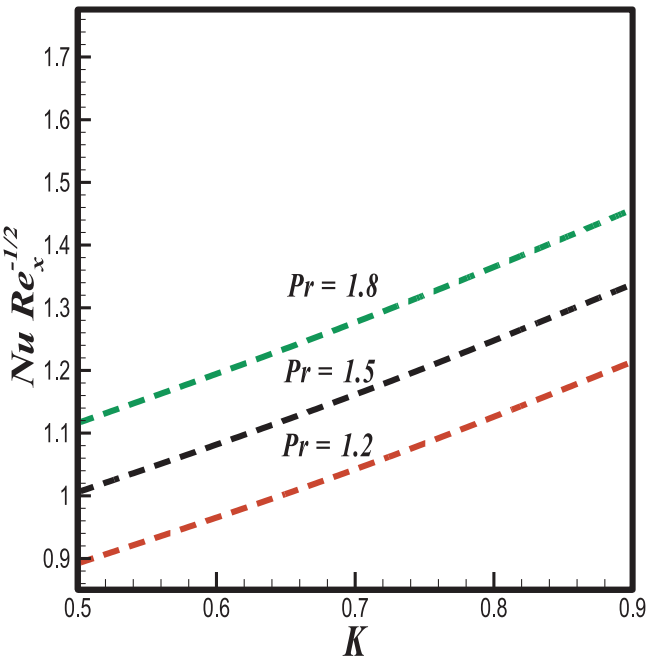

Fig. 9a. Fluctuation of Nusselt number due to Pr *and* K.

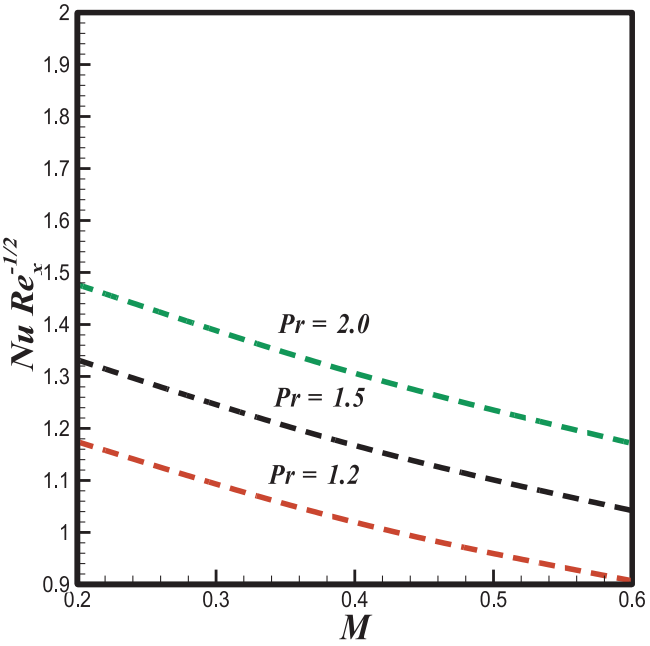

Fig. 9b. Fluctuation of Nusselt number due to Pr *and* M.

Table 1
Variation of Skin friction for different values of We,K *and* M.

We	M	$C_f Re_x^{1/2}$ $K = 0.0$	$C_f Re_x^{1/2}$ $K = 0.5$
0.1	0.2	2.1789	1.9402
0.5		2.1909	1.9671
0.8		2.2875	1.9708
	0.2	2.2627	1.7831
0.1	0.4	2.4692	1.8240
	0.6	2.5748	1.9561

Table 2
Variation of Nusselt number for different values of Pr,K *and* M.

Pr	K	M	$Nu Re_x^{-1/2}$
1.2	0.2	0.2	1.1744
1.5			1.3319
1.8			1.4770
1.2	0.5		1.5630
	0.7		1.8516
	0.9		2.1591
	0.2	0.2	1.1744
		0.4	1.0196
		0.6	0.9069

Table 3
Variation of Nusselt number for different values of Pr*and* S.

Pr	S	$\frac{Nu}{Re_x^{\frac{1}{2}}}$ $K = 0.0$	$\frac{Nu}{Re_x^{\frac{1}{2}}} K = 0.5$
0.5	0.2	1.2581	1.1744
0.8		1.3436	1.3319
1.0		1.5942	1.4770
	0.5	1.6327	1.5630
0.5	0.8	1.4321	1.3894
	1.0	1.2259	1.1863

Conclusion

Current analysis is dedicated to analyze two-dimensional steady flow of MHD Carreau fluid over a stretching cylinder with stratification aspects. The governing non-linear boundary value problem is solved by using shooting method. The main outcomes are listed below:

1) The velocity profile enhances for shear thinning fluids while it shows opposite behavior for shear thickening fluids in case of large value of Weissenberg number.
2) Curvature parameter tends to decline the temperature of fluid flow both in attendance and absence of thermal stratification.
3) Magnitude of Skin friction coefficient in absolute sense is comparatively higher in case of stretching sheet ($K = 0.0$) and for cylinder ($K = 0.5$).

Appendix A. Supplementary data

Supplementary data associated with this article can be found, in the online version, at http://dx.doi.org/10.1016/j.rinp.2018.05.005.

References:

[1] Carreau PJ. An analysis of the viscous behavior of polymer solutions. Can J Chem Eng 1979;57:135140.
[2] Olajuwon BI. Convection heat and mass transfer in a hydromagnetic Carreau fluid past a vertical porous plate in presence of thermal radiation and thermal diffusion. Therm Sci 2011;15:241–52.
[3] Pantokratoras A. Non-similar Blasius and Sakiadis flow of a non-Newtonian Carreau fluid. J Taiwan Inst Chem Eng 2015;56:1–5.
[4] Shadid JN, Eckert ERG. Viscous heating of a cylinder with finite length by a high viscosity fluid in steady longitudinal flow, Non-Newtonian Carreau model fluids. Int J Heat Mass Transf 1992;35:39–49.
[5] Khellaf K, Lauriat G. Numerical study of heat transfer in a non-Newtonian Carreau-fluid between rotating concentric vertical cylinders. J Non-Newton Fluid Mech 2000;89:45–61.
[6] Raju CSK, Sandeep N. Falkner-Skan flow of a magnetic-Carreau fluid past a wedge in the presence of cross diffusion effects. Eur Phys J Plus 2016;131:267.
[7] Khan M, Hashim. Boundary layer flow and heat transfer to Carreau fluid over a nonlinear stretching sheet. AIP Adv 2015;5:10723.
[8] Akbar NS, Nadeem S, Haq RU, Ye S. MHD stagnation point flow of Carreau fluid toward a permeable shrinking sheet: dual solutions. Ain Sha Eng J 2014;5:1233–9.
[9] Hashim M Khan. On Cattaneo–Christov heat flux model for Carreau fluid flow over a slendering sheet. Results Phys 2017;7:310–7.
[10] Khan M, Hashim M, Hussain M. Azam, Magnetohydrodynamic flow of Carreau fluid over a convectively heated surface in the presence of non-linear radiation. J Magnet Magnet Mater 2016;412:63–9.
[11] Kumar KG, Gireesha BJ, Rudraswamy NG, Manjunatha S. Radiative heat transfers of Carreau fluid flow over a stretching sheet with fluid particle suspension and temperature jump. Result Phys 2017;7:3976–83.
[12] G.R. Mchireddy, S. Naramgari, Heat and mass transfer in radiative MHD Carreau fluid with cross diffusion, Ain Shams Eng J, doi.org/10.1016/j.asej.2016.06012.
[13] Srinivasacharya D, Upendar M. Effect of double stratification on MHD free convection in a micropolar fluid. J Egypt Math Soc 2013;3:370–8.
[14] Mishra SR, Pattnaik PK, Dash GC. Effect of heat source and double stratification on MHD free convection in a micropolar fluid. Alexandria Eng. J. 2015;54:681–9.
[15] Reddy CR, Murthy PVSN, Rashad AM, Chamkha AJ. Numerical study of thermally stratified nanofluid flow in a saturated non-Darcy porous medium. Eur Phys J Plus 2014;129:25–34.
[16] Ibrahim W, Makinde OD. The effect of double stratification on boundary-layer flow and heat transfer of nanofluid over a vertical plate. Comput Fluids 2013;86:433–41.
[17] Abbasi FM, Shehzad SA, Hayat T, Alhuthali MS. Mixed convection flow of Jeffrey nanofluid with thermal radiation and double stratification. J Hydrodynamics 2016;5:840–9.
[18] Hayat T, Shehzad SA, Al-Sulami HH, Asghar S. Influence of thermal stratification on the radiative flow of Maxwell fluid. J Braz Soc Mech Sci Eng 2013;35:381–9.
[19] Farooq M, Javed M, Khan MI, Anjum A, Hayat T. Melting heat transfer and double stratification in stagnation flow of viscous nanofluid. Result in Physics 2017;7:2296–301.
[20] Farooq M, Anzar QA, Hayat T, Khan MI, Anjum A. Local similar solution of MHD stagnation point flow in Carreau fluid over a non-linear stretched surface with double stratified medium. Result in Physics 2017;7:3078–89.
[21] Vajravelu K, Prasad KV, Santhi SR. Axisymmetric magneto-hydrodynamic (MHD) flow and heat transfer at a non-isothermal stretching cylinder. Appl Math Comput 2012;219:3993–4005.
[22] Mukhopadhyay S. MHD boundary layer slip flow along a stretching cylinder. Ain Shams Eng J 2013;4:317–24.
[23] Ibrahim Wubshet. Nonlinear radiative heat transfer in magnetohydrodynamic (MHD) stagnation point flow of nano fluid past a stretching sheet with convective boundary condition. Propul Power Res 2015;4:230–9.
[24] Sohut NFHM, Aziz AS, Ali ZM. Double stratification effects on boundary layer over a stretching cylinder with chemical reaction and heat generation. J Phys 2017;890:012019.
[25] Salahuddin T, Hussain A, Malik MY, Awais M, Khan M. Carreau nanofluid impinging over a stretching cylinder with generalized slip effects: Using finite difference scheme. Result in Physics 2017;7:3090–9.